Remotely-piloted aerial system for photogrammetry: orthoimage generation for mapping applications

JŪRATĖ SUŽIEDELYTĖ VISOCKIENĖ[1], DOMANTAS BRUČAS[2], RENATA BAGDŽIŪNAITĖ[1], RŪTA PUZIENĖ[1], ARMINAS STANIONIS[1], UGNIUS RAGAUSKAS[1]

[1] Vilnius Gediminas Technical University, Sauletekio av. 11, Vilnius, LT-10223, Lithuania; e-mail: jurate.visockiene@vgtu.lt
[2] Space Science and Technology Institute, Sauletekio av. 15, Vilnius, LT-1023, Lithuania

ABSTRACT Recently the tendency of replacing aircraft by light, simple, cheap unmanned aerial vehicles for the purposes of updating the field of aerial photogrammetry has been observed. The article deals with the issues of project calculations concerning unmanned aerial vehicles flights and an analysis of the images acquired during field-testing flights. In this article, we analyze the images acquired by mini unmanned aerial vehicles, in particular, the 1.8 plane and the plane SOA-1 that have been processed by a commercial off-the-shelf software package Agisoft PhotoScan (Russia). The 1.8 plane was equipped with the camera Canon S100, containing known camera calibration parameters. These parameters were used for the processing of the image. The aircraft SOA-1 had the camera Canon PowerShot SX280 HS without camera calibration parameters. The camera parameters were calculated by software during the processing image. The paper also presents results of an investigation into the average camera location errors during the test flights, the quality of orthoimage generation by point cloud and a digital terrain model.

KEY WORDS unmanned aerial vehicle – photogrammetry –mission planning – orthoimage

SUŽIEDELYTĖ VISOCKIENĖ, J., BRUČAS, D., BAGDŽIŪNAITĖ, R., PUZIENĖ, R., STANIONIS, A., RAGAUSKAS, U. (2016): Remotely-piloted aerial system for photogrammetry: orthoimage generation for mapping applications. Geografie, 121, 3, 349–367.
Received September 2014, accepted February 2016.

1. Introduction

Information about current land-objects and the terrain is important for the land management and the creation of geographic information system (GIS) and accurate land-cover maps of these areas. Thus, the orthoimage map being used has the fundamental meaning and has two basic components – image and symbol. The image component is represented by remote sensing image(s), while the symbol component is represented by cartographical symbols (points, polylines, polygons and text) (Bělka, Voženílek 2014). Orthoimage may be generated from difference types of images. So far, satellite and aerial (implementing manned aircrafts) images have been widely used. Nevertheless, the situation is changing and recently low altitude unmanned vehicles have already been started to be used to obtain high resolution aerial images, what has developed into the separate industry (Cho et al. 2013, Mayr 2013, Petrie 2013). A low altitude-system flies underneath (up to 150 m) the air traffic (Everaerts 2008) and the cloud cover. This system is recognized by the term of Unmanned Aerial Vehicle (UAV). This term has been adopted by the US Department of Defense (DOD) and the Civil Aviation Authority (CAA) of the UK. The International Civil Aviation Organization (ICAO) has introduced the concept of "Remotely-Piloted Aerial System" (RPAS); a particular class of the UAV is placed inside of the RPAS. This term has been grounded by the fact that only RPAS will be able to integrate into the international civil aviation system as low-altitude imaging system UAV (Colomina, Molina 2014). The UAV, the ground control station and the communication data link (autopilots, navigation sensors, imaging sensors, mechanical servos, and wireless systems) are the components of the RPAS. There are UAVs of different models, characteristics, sizes, weights and other features (Laliberte et al. 2010). The ground control stations are hardware/software devices used for planning the flight of the unmanned aircraft during the flight or previously. Ground control stations are probably as important as the unmanned aircraft themselves, as they enable the interface with the "human intelligence" – any change in the route of the UAVs, any eventual error on the aerial platform or any outcome of the payload sensors shall be sent to and seen within the ground control station (Colomina, Molina 2014). The RPAS components are shown in the Figure 1.

There are lots of constructions of unmanned aircrafts, GSCs and the communication data links in Europe. In the component of RPAS – control station and data link – the mission preparation and its execution are not explicitly mentioned (Mayr 2011). It is very important to gain the experience and the rate for the design of the aircraft trajectory (waypoints, strips, speed, attitude, etc.) and the capacity of the flexible real-time mission management (sensor configuration, triggering events, flying directions, etc.). This data link influences the quality of the image. The images can be used for orthoimages or mosaicking purposes and they can be

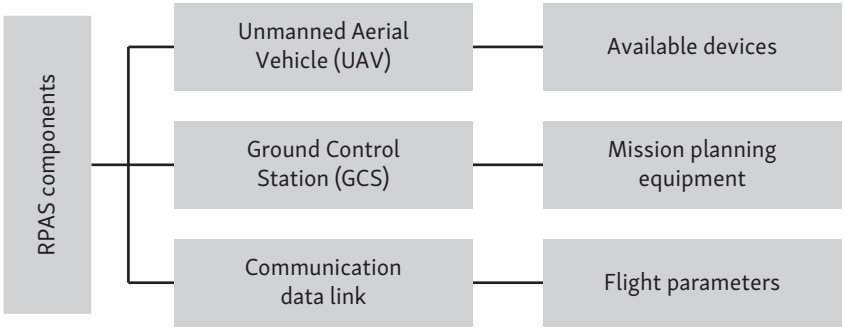

Fig. 1 – Components of RPAS

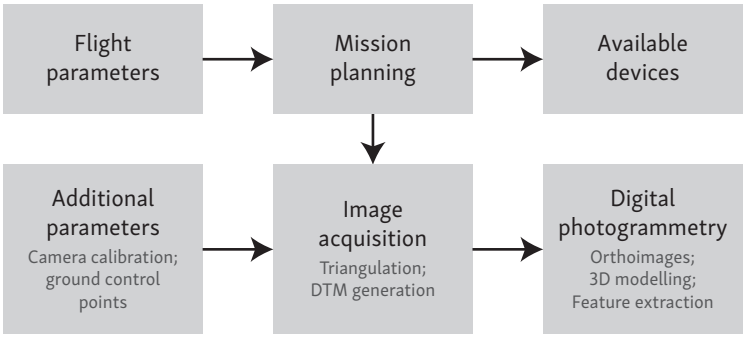

Fig. 2 – Workflow of processing UAV images

the input to the photogrammetric processes. The workflow of processing UAV images are shown in the Figure 2.

The scientists and engineers of Space Science and Technology Institute (SSTI) and the researchers of A. Gustaitis Aviation Institute (AGAI) are working on the RPAS in Lithuania, too. Land-cover and orthoimage mapping, updating of maps for military, geography and civil or scientific applications were of the main purpose for constructing these kinds of systems. The landscape or detailed land-cover maps would be created basing on the orthoimage maps data.. The advantages of using the RPASs for orthoimage mapping (imaging) are obvious: low cost of the system and its exploitation; high flexibility of the system; higher probability of acquiring the images despite weather conditions; possibility of implementation of the systems in case the manned aircraft may not be used (in great variety of applications) (Brucas et al. 2013, Bertacchini et al. 2014). Another advantage of the orthoimage-based data acquisition is the opportunity for land-cover mapping at fine resolution. The increased sophistication in image processing should be incorporated to achieve high mapping/classification accuracy from high-resolution images (Li, Shao 2014). Several models of fixed wing aircrafts, the X5 plane and the 1.8 m plane have been

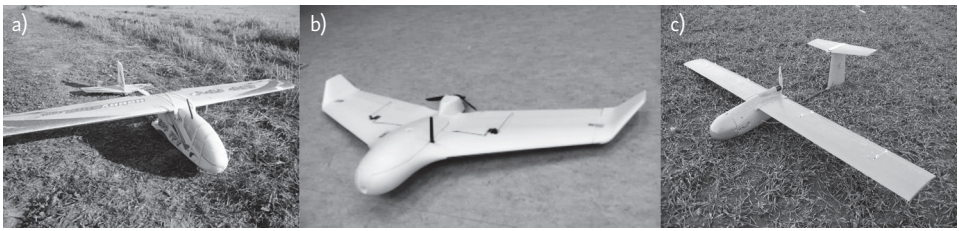

Fig. 3 – Models of aircrafts: a – 1.8 m plane, b – X5, c – "Buzzard" (SOA-1)

tested, both of them based on readily available foam RC model sets (Fig. 3a, b). Both aircrafts are similar in respect of the payload; however, the X5 plane has lower take-off weights, higher speed, and better endurance due to its tailless (flying wing) configurations. These aircrafts can be considered as the category of MINI UAVs (MUAV; Gupta, Ghonge, Jawandhiya 2013; Eisenbeiss 2004). These are the vehicles weighting in range of 2–20 kg, normal operating altitude up to 900 m, radius of mission – 25 km. This aircraft (Fig. 3a) is able to cover 3.5–5 km² of area during one flight, the maximum speed of the flight is 70 km/h and the flying time is approx. 45 min.

As the result of the initial testing in real time environment (UAV platforms mentioned before) a new fully composite MUAV platform "Buzzard" (SOA-1) has been developed in order to ensure the better flight stability, ease of exploitation, durability and wind tolerance. The platform itself ensures simple hand launch with belly landing, which is far less sensible to launching conditions (compared to X5 platform), thus ensuring sufficient wind tolerance (up to 10 m/s), high cruise speed (up to 20 m/s) and greater robustness (compared to 1.8 m aircraft). The "Buzzard" aircraft has the total take-off weight in range of 4 kg, payload of up to 0.7 kg, cruise speed in range of 70 km/h, and flight endurance of up to 2 h. The platform also ensures simple and convenient replacement of payloads (cameras), ensuring the possibility of implementation of various camera payloads on the same UAV platform (Fig. 3c).

The MUAV had an installed *Canon S100* digital camera used for test flights. The camera lens optics was calibrated by the specified German program *Tcc* according to the calibration stand – cube. The size of the digital matrix of the image taken by the camera *Canon S100* is 7.44 × 5.58 mm, thus, the smallest size of the image pixel size is 0.00186 mm. The focal length is 5.361 mm (Sužiedelytė-Visockienė 2012; Sužiedelytė-Visockienė, Bručas 2009; Sužiedelytė-Visockienė, Bručas, Ragauskas 2014).

The accuracy of the camera calibration is characterized by the standard deviation (δ_0) of the weight unit, which indicates the accuracy of the identification and measurement of the points on the calibration stand. Theoretically, this value does not have to exceed 15 μm. After calibration of camera *Canon S100*, the standard

deviation of the weight unit was 3.16 μm; the acquired result is acceptable (Kiseleva 2002, Schenk 2005).

The results of test flights and the orthoimaging by the 1.8 m plane and SOA-1 plane are further described in the paper.

2. Mission planning

One of the components of the mission planning is flight planning. It is one of the basic photogrammetric project stages. Projected boundaries of the area; model of the camera integrating to aircraft and calibration result; expected scale of taking images; forward and side overlapping of UAV images; flight direction, speed, height – altitude and data coordinate system are the data of the photogrammetric project (Demirel, Akdeniz, Aksu 2004).

The camera focal length and the altitude of the aircraft flight determine the scale of the UAV image. The classical calculation formula of the areal image scale is the following (Albertz, Kreiling 1989):

$$M_b = 1 : m_b = \frac{c_k}{h_g}, \tag{1}$$

where m_b – an image scale denominator; c_k – the camera focal length; h_g – the flight altitude of the aircraft.

These values have to be considered and calculated when planning the UAV flight. The flight altitude can be obtained from Ground Sample Distance (GSD) and depends on the camera focal length, camera sensor width and on the distance covered on the ground by one image (Quality report Help 2015):

$$c_k = \frac{c_{35} \times S_w}{34.6}, \tag{2}$$

$$\frac{c_k}{h_g} = \frac{S_w}{D}, \quad h_g = \frac{c_k \times D}{S_w}, \tag{3}$$

where c_{35} – focal length in 35 mm equivalent; S_w – sensor width; D – distance covered on the ground by one image.

Normally, the altitude above the ground level (AGL) is taken into consideration, while orthoimaging by MUAVs is normally performed at small areas where ground elevation changes are minor. In case of hilled surface (like mountains etc.) the flight might be planned with required altitude changes based on free of charge Google ground level model. The distance covered on the ground by one image is given by the desired GSD and image size (Quality report Help 2015):

$$D = imW \times GSD, \tag{4}$$

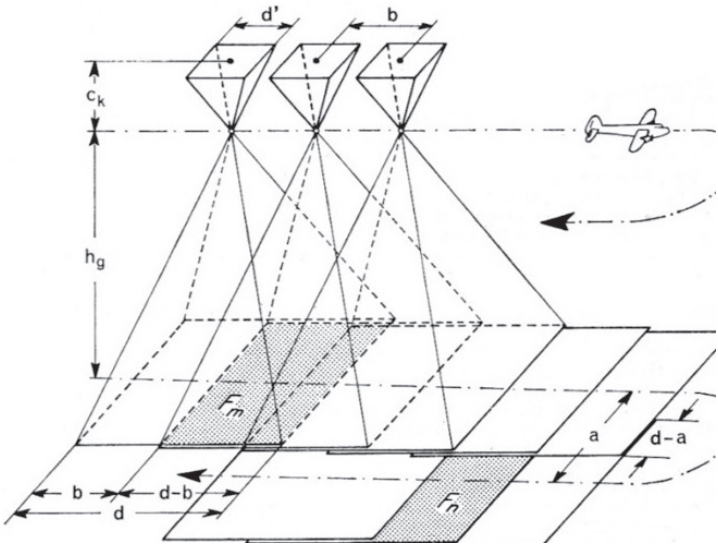

Fig. 4 – Flight project scheme

$$h_g = \frac{c_k \times imW \times GSD}{S_w \times 100}, \tag{5}$$

where *imW* – image width in pixel; *GSD* – desired resolution (cm/pixel).

The theoretical planning of the UAV flight is justified by the calculation of the arrangements of the images along the flight strip. The scheme of the flight project is given in Figure 4 (Albertz, Kreiling 1989).

In the scheme (Fig. 4) *d* – is the size of the image; *p* – is the forward overlapping of the adjacent images on the flight strip; *b* – the base for taking images (the distance between the adjacent centres of the images); *q* – a side overlapping of the images between the upper and lower flight strips.

The image size *d* depends on the camera resolution. During the flights specially modified *Canon S100* camera ensuring triggering by autopilot was used, the maximum resolution of the camera was 12.1 mega pixels. The 4,000 × 3,000 pixel image was acquired (7.44 × 5.58 mm). One has to know the size of the image when calculating the forward and side overlapping of the images during the flight. The formula for the calculation is (Albertz, Kreiling 1989):

$$p = \frac{d - b}{d} \times 100, \tag{6}$$

$$q = \frac{d - a}{d} \times 100. \tag{7}$$

Where *a* – is the distance between the adjacent flights calculated according to this formula:

$$a = d \times \left(1 - \frac{q}{100}\right). \tag{8}$$

The project values of the UAV flights were calculated according to formulas 5–8 taking images by *Canon S100* camera and under ideal flight conditions. The obtained results are given in Table 1.

The flight project parameters are required so not a single area of the investigated location is left without being captured, between the adjacent images and strips, during the process of aircraft flying and taking images of the determined location. When selecting the photogrammetric project parameters it is necessary to take into consideration certain weather conditions during the flight and especially the wind direction (Teets et al. 1998).

The recommended flight direction is East-West or North-South. The images taken while keeping to the mentioned above flight direction are easy to process by the photogrammetric method. However, if needed, the direction is possible to be changed.

Based on the parameters of the photogrammetric project and on the values of the flight project (Table 2), the UAV flight mission could be indicated using the software (*Mission Planner*) during the flight or previously, when indicating the initial and final points of the planned flight strip on the *Google Earth* map

Tab. 1 – Flight project parameters, when used camera *Canon S100*

1 : m_b	h_g, m	d, m	b, m when p = 70%	a, m when q = 45%	a, m when q = 60%
1:2,000	107	149 × 112	45	61	45
1:2,500	134	186 × 140	56	77	56
1:3,000	161	223 × 167	67	92	67
1:3,500	188	260 × 195	78	107	78
1:4,000	214	298 × 223	89	123	89
1:4,500	241	335 × 251	100	138	100
1:5,000	268	372 × 279	112	153	112
1:5,500	295	409 × 307	123	168	123

Tab. 2 – Information about flight parameters

Object-city	Aircraft	Flight altitude, m	Number of images	Coverage area, sq km
Vilnius (Antakalnis)	1.8 plane	220	153	1.03
Kedainiai	1.8 plane	211	90	1.37
Klaipeda	1.8 plane	210	189	1.61
Vilnius (Kirtimai)	1.8 plane	198	50	0.37
Melagenai	1.8 plane	218	164	1.09
Vinius (Totoriu 40)	SOA-1	115	391	0.72

(Mission Planning Software User's Guide 2004). Thus, the beginnings and ends of the geodetic coordinate points of the strip appear on the screen or, to be more exact, on the tables of the software.

During the tests, the flight was planned by implementing the above mentioned *Mission Planner* ground control station software, allowing automated calculation of images' overlaps and triggering time depending on flight parameters. The triggering at the needed points was ensured by the autopilot installed in the aircraft (3DR Pixhawk) depending on the obtained flight distance, but disregarding the aircraft attitude (at particular moment). This ensures obtaining of the sufficient overlapping of images, though images on the corners of the area of interest might be useless due to the turning of the aircraft (high angles of attitude), those images have to be omitted during later processing.

The imaging rate to get the needed overlap depends on the speed of the UAV aircraft. The time between the two images is given by formula (Quality report Help 2015):

$$t = \frac{imH \times GSD \times 0.01 \times (1 - p)}{v}, \tag{9}$$

were t – time between two images in s; imH – image height in pixels; v – flight speed m/s.

During the process of acquiring images, the coordinates of the image centres are determined by GNSS (Global Navigation Satellite System), which can be applied for the photogrammetric measurements of the images in the later stages. The collected GNSS data can be helpful for the extraction of automated tie point and may allow the direct geo-referencing of the captured images (Nex, Remondino 2014), otherwise the ground control points (GCP) are needed. After the image acquisition without GCP the orthoimage must be transformed into the reference coordination system. The special photogrammetric system (PhotoMod) does not generate orthoimages without GCP (PhotoMod 2014).

The general declared accuracy of images' position determination (by means of installed GPS receiver) is in the range of ± 5 m, though normal accuracy determined during experiments do not exceed ± 2 m in case of unprocessed images. After processing of the images (stitching) the final accuracy of photo model has been determined to be in the range of 0.5 m without additional ground control points (GCPs). Implementation of additional GCPs ensure the general accuracy of the model to 3–4 cm.

3. Results of orthoimage generation

RPAS can be used for the purposes of surveying city areas in Lithuania for land-cover mapping (geographic) and cartographic application. Information about flights is shown in the Table 2. We flew 1.8 plane and SOA-1 aircrafts over the test areas in with a 70% forward and 60% side overlap; we used direct geo referencing technique (without GCP) – GNSS data. The 1.8 plane had the integrated camera Canon S100. The camera Canon S100 calibration parameters have the input to the image acquisition software (c_k = 5.365 mm) and can be used to constrain the bundle adjustment. Canon PowerShot SX280 HS was integrated into SOA-1 aircraft, this camera was not calibrated. Camera calibration and image orientation are two fundamental prerequisites for any metric reconstruction from images (Sužiedelytė-Visockienė, Bručas, Ragauskas 2014). Canon PowerShot SX280 HS calibration process was computed by software during the image processing – bundle adjustment time (self-calibration).

The acquisition of images was accomplished by the commercial off-the-shelf software package Agisoft PhotoScan (Russia). The main stages of image acquisition are described below (Agisoft PhotoScan 2015; Singh, Jain, Mandla 2014; Fig. 5).

1. Camera alignment. The photogrammetric system searches for the common points on images and matches them, as well as finds the position of the camera for each image and refines camera calibration parameters. As a result a sparse point cloud and a set of camera positions are formed. The sparse point cloud represents the results of the image alignment and will not be directly used in the further 3D model construction procedure.
2. Building of dense point cloud. Based on the estimated camera positions and images themselves a dense point cloud is built by the software. The dense point cloud may be edited and classified prior to export or proceeding to 3D mesh model generation.
3. Building of mesh. Software reconstructs a 3D polygonal mesh representing the object surface based on the dense point cloud. Additionally there is a Point Cloud method used for the fast geometry generation and based on the sparse point cloud alone. Generally, there are two algorithmic methods available in PhotoScan that can be applied to 3D mesh generation: Height Field – for planar type surfaces, Arbitrary – for any kind of object.
4. After geometry (i.e. mesh) is reconstructed, it can be textured and/or used for orthoimage and DTM generation.

The image acquisition by Agisoft PhotoScan is a fully automated process.

First works of image processing were performed by implementing all of the available images (Table 3). Differences between the image geotags (GNSS) and the optimized camera parameters were obtained. This indicates the quality of the geo-tagging of the original images. The average camera location errors were

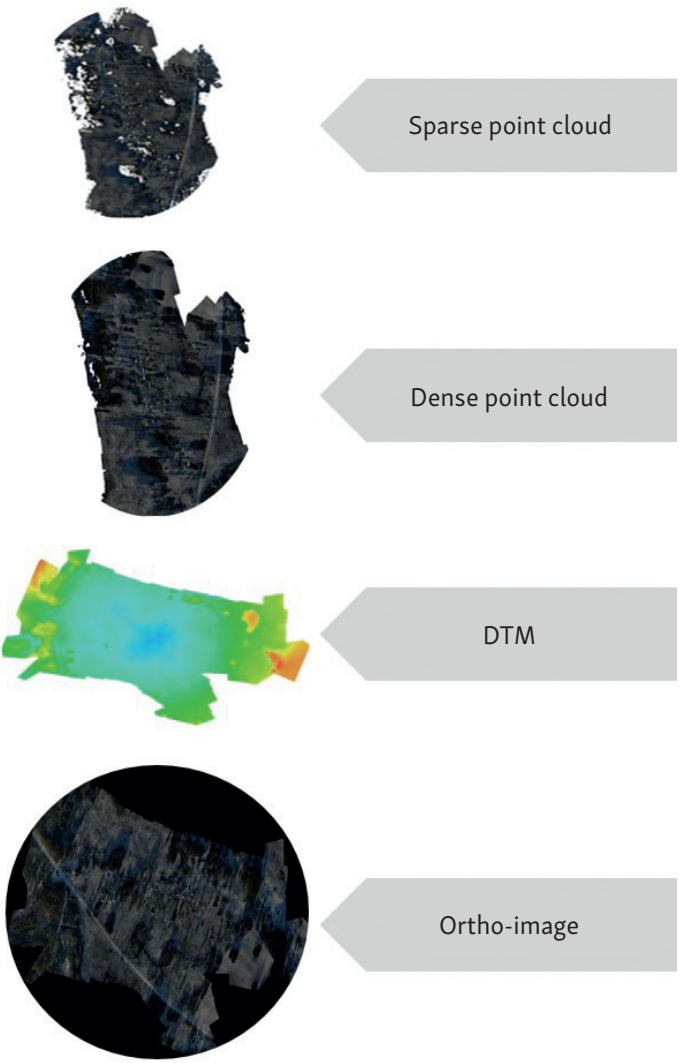

Fig. 5 – Image acquisition process

worse. High values may indicate the presence of such factors as high noise in the GNSS device, poor synchronization with the camera or errors in the geotagging process (Quality report Help 2015). High errors may also arise when images are taken at the moment of aircraft turning to the next strip or crossing all the strip and some images were without GNSS data. It has been noticed that some of the images were taken at high camera roll angles (due to aircraft attitude changes). Such unsuitable images were removed from the project and the image processing was repeated again. The results have improved by as much as 80% in some cases (Table 3).

Tab. 3 – Average camera location error

Object	Vilnius (Antakalnis)			
Number of images	X error, m	Y error, m	Z error, m	Total error, m
35	24.09	5.14	3.53	24.89
28	22.52	4.94	2.71	23.22
Object	Kedainiai			
Number of images	X error, m	Y error, m	Z error, m	Total error, m
90	47.44	89.57	29.49	105.56
72	7.93	9.93	4.31	13.42
Object	Klaipeda			
Number of images	X error, m	Y error, m	Z error, m	Total error, m
189	25.89	24.70	7.98	36.66
149	12.52	10.26	2.78	6.43
Object	Vilnius (Kirtimai)			
Number of images	X error, m	Y error, m	Z error, m	Total error, m
50	18.02	8.10	7.05	20.98
Object	Melagenai			
Number of images	X error, m	Y error, m	Z error, m	Total error, m
164	18.01	8.11	7.05	20.97
104	20.40	4.40	5.02	21.47
Object	Vilnius (Totoriu 40)			
Number of images	X error, m	Y error, m	Z error, m	Total error, m
391	27.87	10.46	10.11	31.44

There were five flight strips in Vilnius (Antakalnis) project in total. Only three strips have left after the removal of the irrelevant images. The first and the last strips were totally removed. The error estimation has remained practically unchanged after the image processing (Table 3, Fig. 6).

In Kedainiai project the first strip was removed, since 7 images had no GNSS data. Similarly, the images of the last strip were also deleted. The total error of the camera position has icreased from 105 to 13 m (Table 3, Fig. 7).

In Klaipeda project the direction of images was reversed, and the part of images containing greatest camera position errors were removed. The quality of the results has increased by 3 times (Table 3, Fig. 8). The object is located on the seaside; therefore, there might be too windy for obtaining sufficient results.

In Melagenai object after removing the images taken during the start of the takeoff till the flight route and at the corners of the route, the result of the decrease of the camera position error from 22 to 14 m (Fig. 9) has been obtained. The strip from the takeoff till the flight route is considered to be a Single track, Single track flight plans are not recommended as they might lead to distorted or incomplete reconstruction (Quality report Help 2015).

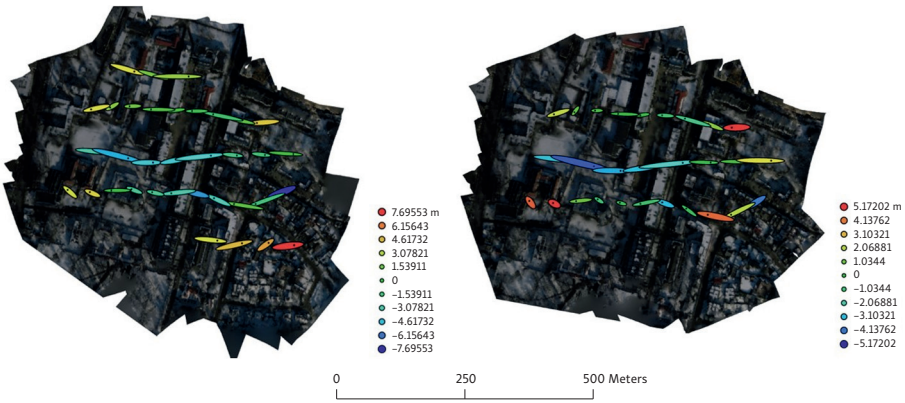

Fig. 6 – Camera locations and error estimates in the Vilnius (Antakalnis)

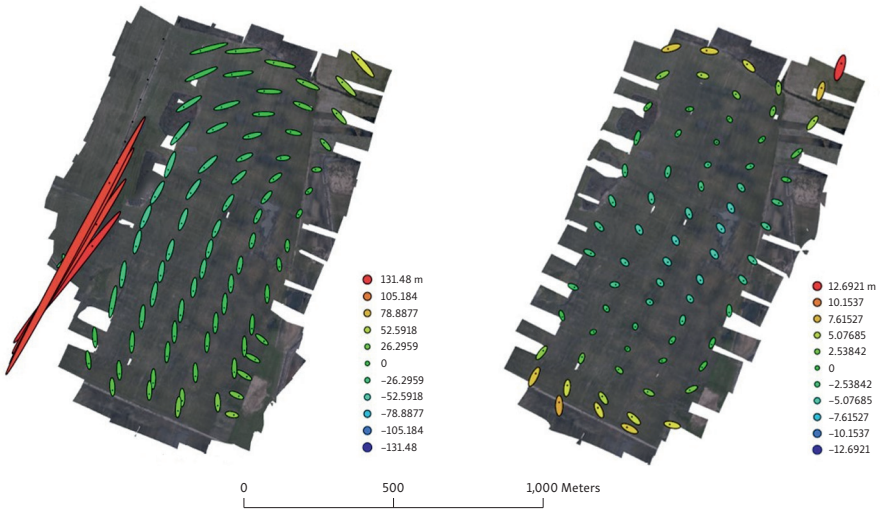

Fig. 7 – Camera locations and error estimates in the Kedainiai

The Kirtimai object was not recalculated because the results obtained the after the processing of images were similar to the results of all other objects (Table 3, Fig. 9).

The images of the Vilnius (Totoriu 40) object were taken by using uncalibrated Canon PowerShot SX280 HS being installed in the SOA-1 aircraft. The results obtained are practically identical to the ones of other projects. Camera locations and error estimations are shown in Table 3 and Figure 10.

The results of the research show that the quality and the accuracy of the results directly depend on the quality and the accuracy of the input images (Quality

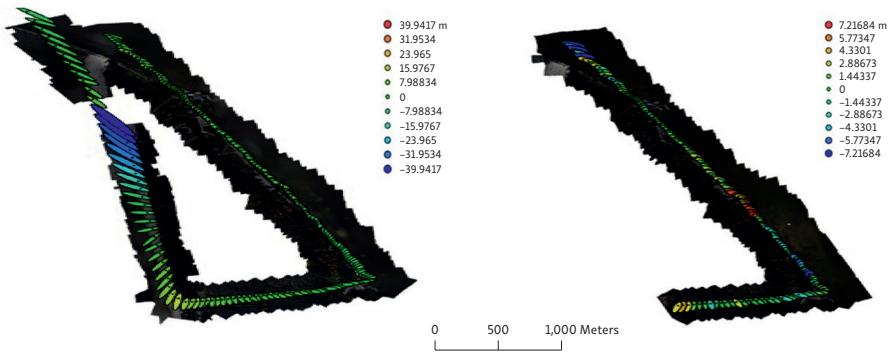

Fig. 8 – Camera locations and error estimates in the Klaipeda

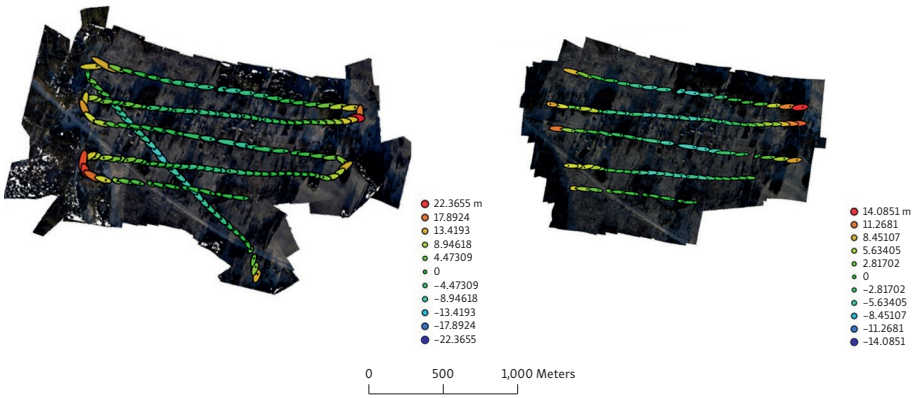

Fig. 9 – Camera locations and error estimates in the Melagenai

report Help 2015). High quality images can be obtained only by correct planning of the flight parameters (2nd chapter). The post processing of images, even if took long computing time (from some hours to more than 12 for each set) allowed the extraction of very important information derived from the 3D models obtained (Bělka, Voženílek 2013). The high quality and speed computer equipment could be precipitate the image acquisition time.

The resulting accuracies of RPAS (2–10 m position accuracy and 0.5–5 deg attitude accuracy) can be insufficient for some applications. In contrast, high precision direct georeferencing of UAVs by the means of differential GPS (DGPS) techniques, such as Real Time Kinematic (RTK) GPS, may lead to the position accuracy better than 5 cm (Eling et. al. 2013).

After the processing of the images by Dens cloud point and DTM results the orthoimages have been generated. The quality results are shown in the Table 4.

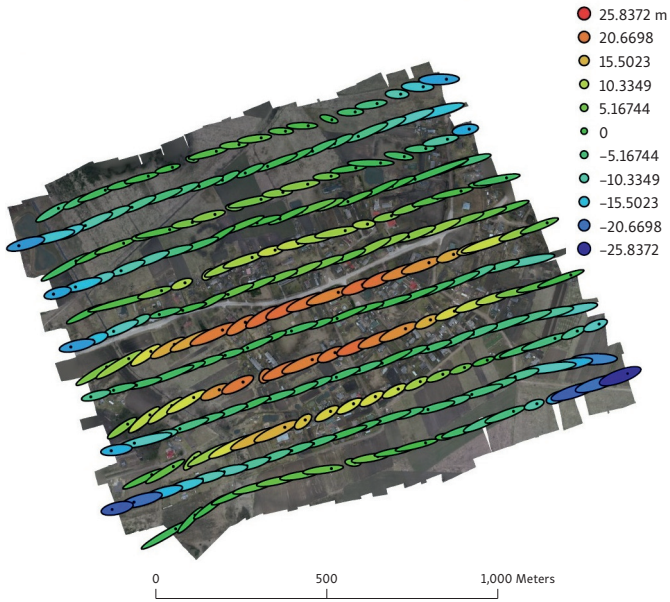

Fig. 10 – Camera locations and error estimates in the Vilnius (Totoriu 40)

The accuracy of the results can be evaluated by importing orthoimages to Google Earth maps. The greatest deviations appeared in the Vilnius (Kirtimai) object, what is evident from the Table 4. The orthoimage error is in range of 10 pixels.

All the results of orthoimages are available on the Internet site www.landimage.eu. The example of the latest orthoimage of the object Vilnius (Totoriu 40) is shown on the site and in Figure 11. The orthoimage error is 29 μm (Table 4). The least error of the orthoimage is in the Kedainiai and Klaipeda objects, and it is under 15 μm.

There is a possibility to analyse the land-cover changes by comparing the available information with latest orthoimage maps. There is a possibility to demonstrate the matching of available orthoimage map of Vilnius (40 Totoriu vl.)

Tab. 4 – Quality results of orthoimage generation

Object	Ground resolution, m/pix	DTM resolution, m/pix	Orthoimage error, pix	Orthoimage error, mμ
Vilnius (Antakalnis)	0.065	0.26	1.13	20
Kedainiai	0.063	0.25	0.83	15
Klaipeda	0.064	0.26	0.69	13
Vilnius (Kirtimai)	0.061	0.12	10.42	190
Melagenai	0.066	0.26	1.06	19
Vilnius (Totoriu 40)	0.032	0.12	1.60	29

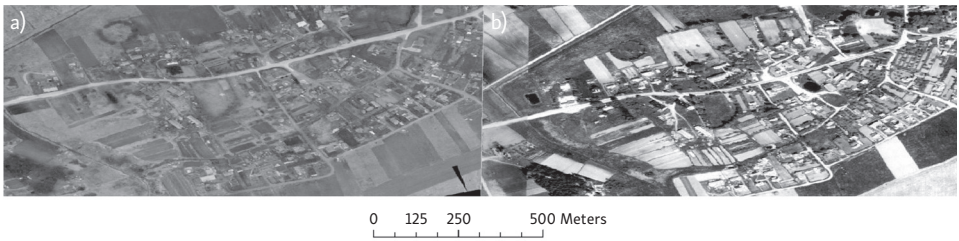

Fig. 11 – Orthoimage of the object in Vilnius (Totoriu 40): a – from UAV, b – made in 1995

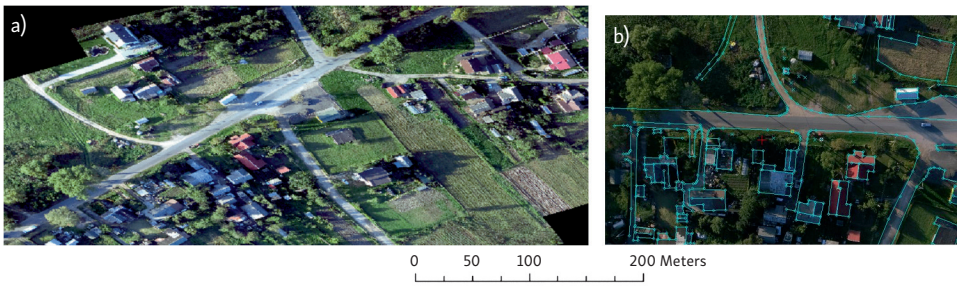

Fig. 12 – Example of: a – orthoimage; b – orthoimage map

made in 1995–2000 (www.geoportal.lt) with the compiled new orthoimage from UAV (Fig. 11). There is a possibility to calculate the index of land changes (IC) by following formula (Kupková, Bičík, Najman 2013):

$$IC = \frac{\sum_{i=1}^{n} A_{1i} - A_{2i}}{2 \times E} \times 100, \tag{10}$$

where A_{1i} – the aerial extend of ith land use category in first year; A_{2i} – the aerial extend of ith land use category in second year; E – total aerial extend of analysed land.

There is a possibility of simple and quick update of the databases of the digital maps, after the substantial changes in the terrain of the investigated area by means of the new AGAI and SSTI technology. Results presented in the Table 4 show UAV orthoimage supply high quality data for geographic analysis.

The orthoimage of the area made by the photogrammetric method is considered to be the basis of the data collecting for the orthoimage map, for the vector type-cartographic and for three-dimensional spatial data. The example of an orthoimage and an orthoimage map made by stereo pairs are shown in the Figure 12 (Kirtimai territory).

4. Conclusions

The flight route project has to be worked out before each flight in order to avoid omitting any not captured location. The weather conditions have to be taken into account when planning the workflow of the future flight, as they can influence the results quite considerably. The terrain orthoimages may be made available for the analysis of the environment modifications and economical changes of the location, when comparing the information collected under the field conditions on a certain locality with the latest acquired cartographic material.

Implementation of different kinds of aircrafts (more stable and less prone to wind) does not ensure better quality of imaging data, nonetheless it ensures flight possibilities under wider range of climatic conditions. In case of careless or unsuitable mission planning imaging data might have to be corrected manually to obtain suitable results. That increases the labour hours needed to produce suitable orthoimage maps. In order to ensure obtaining of the results, the best is to implement automated flight and imaging planning procedures on ground control station.

For the purposes of upgrading the orthoimage map databases and fixation of land cove changes in a simple and fast way after the substantial modifications of the location have been made, the newly constructed by SSTI and AGAI technology is recommended to be used. The specific climatic conditions, especially clouds and fogs, prevent from acquiring high quality images on the territory of Lithuania. These disturbances are not significant for unmanned aerial vehicles, flying at altitudes under 300 m.

References

ALBERTZ, J., KREILING, W. (1989): Photogrammetric guide. Karlsruhe, Wichmann.

BĚLKA, L., VOŽENÍLEK, V. (2014): Prototypes of orthoimage maps as tools for geophysical application. Pure nad Applied Geophysics, 171, 6, 1047–1059, DOI 10.1007/s00024-013-0665-y.

BERTACCHINI, E., CASTAGNETTI, C., CORSINI, A., DE CONOA, S. (2014): Remotely piloted aircraft systems (RPAS) for high resolution topography and monitoring: civil protection purposes on hydrogeological contexts. Conference paper in proceedings of SPIE – the international society for optical engineering, DOI: 10.1117/12.2067406.

BRUCAS, D., SUZIEDELYTE-VISOCKIENE, J., RAGAUSKAS, U., BERTESKA, E., RUDINSKAS, D. (2013): Testing and implementation of low cost UAV platform for orthophoto imaging. ISPRS Archives, XL–1/W2, 55––59.

CHO, G., HILDEBRAND, A., CLAUSSEN, J., COSYN, P., MORRIS, S. (2013): Pilotless aerial vehicle systems: size, scale and functions. Coordinates, 9, 1, 8–16.

COLOMINA, I., MOLINA, P. (2014): Unmanned aerial systems for photogrammetry and remote sensing: A review. ISPRS Journal of Photogrammetry and Remote Sensing, 92, 79–97.

DEMIREL, A.S., AKDENIZ, H., AKSU, O. (2004): Two functional software for internal use; flight planning and Presenting of digital orthophotos. ISPRS Archives, XXXV, B4, 344–347.

EISENBEISS, H. (2004): A Mini Unmanned Aerial Vehicle (UAV): System overview and image acquisition. ISPRS Archives, XXXVI–5/W1, 1–7.
ELING, C.H., KLINGBEIL, L., WIELAND, M., KUHLMANN, H. (2013): A precise position and attitude determination system for Lightweight unmanned aerial vehicles. UAV-g2013, XL-1/W2, 113–118.
EVERAERTS, J. (2008): The use of unmanned aerial vehicles (UAVs) for remote sensing and mapping. ISPRS Archives, XXXVII, B1, 1–6.
GUPTA, S.G., GHONGE, M.M., JAWANDHIYA, P.M. (2013): Review of Unmanned Aircraft System (UAS). International Journal of Advanced Research in Computer Engineering & Technology (IJARCET), 2, 4, 2278–1323.
KISELEVA, A.S. (2002): Accuracy control at various stages of photogrammetric processing in PhotoMod system, http://www.racurs.ru (2.4.2015).
KUPKOVÁ, V., BIČÍK, I., NAJMAN, J. (2013): Land Cover Changes along the Iron Curtain 1990–2006. Geografie, 118, 2, 95–115.
LALIBERTE, A.S., JEFFREY, E.H., RANGO, A., WINTERS, C. (2010): Acquisition, or the rectification, and Object-based Classification of Unmanned Aerial Vehicle (UAV) Imagery for Rangeland Monitoring. Journal of Photogrammetric Engineering & Remote Sensing, 76, 6, 661–672.
LI, X., SHAO, G. (2014): Object-Based Land-Cover Mapping with High Resolution Aerial Photography at a County Scale in Midwestern USA. ISPRS Journal of Photogrammetry and Remote Sensing, 6, 11372–11390.
MAYR, W. (2011): Unmanned aerial systems in use for mapping at BLOM. Photogrammetric Week, 125–134.
MAYR, W. (2013): Unmanned aerial systems – for the rest of us. Photogrammetric Week, 151–163.
NEX, F., REMONDINO, F. (2014): UAV for 3D mapping application: a review. Appl Geomat, 6, 1–15.
PETRIE, G. (2013): Commercial operation of lightweight UAVs for aerial imaging and mapping. GEOInformatics, 16, 1, 28–39.
SCHENK, T. (2005): Introduction to Photogrammetry, http://www.mat.uc.pt/~gil/downloads/IntroPhoto.pdf (22.3.2015).
SINGH, S.P., JAIN, K., MANDLA, R.V. (2014): Image based 3D city modeling: comparative study. ISPRS Archives, ISPRS Technical Commission V Symposium, XL-5, 537–546.
SUŽIEDELYTĖ VISOCKIENĖ, J. (2012): Photogrammetry requirements for digital camera calibration applying Tcc and MatLab software. Journal of Geodesy and Cartography, 38, 3, 106–110.
SUŽIEDELYTĖ VISOCKIENĖ, J., BRUČAS, D. (2009): Influence of digital camera errors on the photogrammetric image processing. Journal of Geodesy and Cartography, 35, 1, 29–33.
SUŽIEDELYTĖ VISOCKIENĖ, J., BRUČAS, D., RAGAUSKAS, U. (2014): Comparison of UAV images processing softwares, Journal of Measurements in Engineering, 2, 2, 96–106.
TEETS, E.H., DONOHUE, C.J., UNDERWOOD, K., BAUER, J.E. (1998): Atmospheric Considerations for Uninhabited Aerial Vehicle (UAV) Flight Test Planning, technical memorandum. Report Number:

Other materials

Agisoft PhotoScan, http://www.agisoft.com, (5.3.2015).
Agisoft PhotoScan User manual (2014), http://www.agisoft.com/pdf/photoscan-pro_1_1_en.pdf (2.5.2015).

Mission Planning Software User's Guide (2004), ftp://ftp.ashtech.com/Spectra-precision/Utility%20Software/Mission%20Planning/Manuals/Mission%20Planning%20User%27s%20Guide%20630115-01%20Rev%20C.pdf (10.3.2015).
PhotoMod 4.4 Overview, user manual (2009), http://www.racurs.ru (12.3.2015)
Quality report Help, http://uav.pix4d.com/static/quality_report_help.pdf (5.3.2015).
NASA-TM-1998-206541, http://www.nasa.gov/centers/dryden/news/DTRS/1998/citation_prt.htm, 1–17 (19.3.2015).

SHRNUTÍ

Dálkově ovládaný letecký systém pro fotogrammetrii: pořízení ortofot pro mapové aplikace

Informace o pozemních objektech a terénu jsou důležité pro územní plánování a tvorbu geografického informačního systému (GIS) a přesných map krajinného pokryvu daných oblastí. Častým výstupem bývá ortofotomapa, jež má dvě základní složky: ortofota a ortografické značky. V současné době lze pořídit fotografie lehkými, jednoduchými a levnými bezpilotními letadly (drony). Tato letadla fungují v rámci dálkově ovládaného leteckého systému (RPAS). Takový systém sestává z pozemní řídící stanice a bezdrátového datového komunikačního spojení s mechanickými ovladači, navigačními čidly a obrazovými snímači umístěnými na palubě dronu. Na tomto vybavení závisí kvalita snímků. Díky aplikaci takovýchto systémů lze rychle pořídit údaje s vysokým stupněm rozlišení u malých oblastí (o ty je největší zájem). Navíc nedávný vývoj u konstrukce a zavádění malých bezpilotních letadel podstatně snížil cenu a velikost těchto systémů, což nám umožňuje jejich velice široké využití. Pro vyhovující fotogrammetrické parametry je však nezbytné provést před letem pozemní projektové naplánování trasy letu – zejména je nutné vybrat náležitou letovou výšku a vzhledem k rychlosti bezpilotního prostředku určit čas pořizování jednotlivých snímků.

Článek pojednává o otázkách sestavení projektu v případě letu bezpilotních letadel a o analýze snímků pořízených během letů v terénu. V článku zkoumáme snímky pořízené miniaturními bezpilotními letadly, zejména letadlem typu 1,8 a letadlem SOA-1, jež zkonstruovali vědci a inženýři z Ústavu kosmonautiky a techniky (SSTI) a badatelé z Leteckého ústavu A. Gustaitise v Litvě. Jsou to přístroje vážící 2 až 20 kg, s normální operační výškou do 900 m a doletem 25 km. Letadlo typu 1,8 je schopno pokrýt během jednoho letu 3,5 až 5 km² plochy při maximální rychlosti 70 km/h a letovém času přibližně 45 minut. Letadlo SOA-1 má celkovou váhu při vzletu zhruba 4 kg, užitečné zatížení až 0,7 kg, rychlost kolem 70 km/h a letový čas až 2 hodiny. Jeho konstrukce také zajišťuje jednoduchou a příhodnou výměnu užitečného zatížení (fotoaparátů) a možnost aplikace různého fotografického příslušenství. Letadlo typu 1,8 bylo opatřeno fotoaparátem Canon S100, jenž obsahuje známé fotografické kalibrační parametry. Tyto parametry byly využity ke zpracování snímků. Letadlo SOA-1 mělo fotoaparát Canon Power Shot SX280 HS bez fotografických kalibračních parametrů. Článek dále přináší údaje o průměrné chybě vzniklé z umístění fotoaparátu a o kvalitě ortofot generovaných množinou bodů a dále digitální terénní model. Litevská bezpilotní letadla lze využívat k účelům průzkumu městských oblastí v Litvě v oblasti mapování krajinného pokryvu (geografické užití), kartografických aplikací a tvorby ortografických map. Let byl podniknut nad zkušebními oblastmi. Použili jsme přímou metodu geografických vztažných bodů (bez geodetických bodů) – údaje globálního navigačního

družicového systému. Snímky byly pořízeny komerčním, na míru sestaveným softwarovým souborem Agisoft PhotoScan (Rusko). Jsou tu ukázány rozdíly mezi parametry u snímků s přidáním geografických metadat (na základě globálního navigačního družicového systému) a snímků s optimalizovanými fotografickými parametry. Vznikají závažné chyby, pokud se snímky pořizují v okamžiku, kdy se letadlo obrací k další letové řadě, když překračuje všechny řady nebo když jsou snímky bez údajů z globálního navigačního družicového systému. Bylo zjištěno, že některé snímky byly pořízeny při změně orientace (v důsledku změn u výšky letadla). Takové nevhodné snímky byly z projektu vypuštěny a zpracování snímků bylo zopakováno. Výsledky se v některých případech zlepšily o 80 %. Výsledky průzkumu ukazují, že kvalita a přesnost závisejí přímo na kvalitě a přesnosti vkládaných snímků. Snímky vysoké kvality lze získat jedině přesným naplánováním letových parametrů. Konečné výsledky, vzešlé z následného zpracování, spočívají ve tvorbě ortofot a ortografických map pomocí vektorových dat, což je plodem digitalizace ortofot. Je tu možnost analyzovat změny krajinného pokryvu srovnáním dostupných informací s posledními ortografickými mapami.

Obr. 1 Složky dálkově ovládaného leteckého systému (RPAS)
Obr. 2 Postup prací při zpracování snímků bezpilotních letadel
Obr. 3 Modely letadel: a – letadlo typu 1,8 m, b – X5, c – „Káně“ (SOA-1)
Obr. 4 Schéma letového projektu
Obr. 5 Proces pořízení snímků
Obr. 6 Umístění fotoaparátu a odhadnutá chyba ve Vilniusu (Antakalnis)
Obr. 7 Umístění fotoaparátu a odhadnutá chyba v Kedainiai
Obr. 8 Umístění fotoaparátu a odhadnutá chyba v Klajpedě
Obr. 9 Umístění fotoaparátu a odhadnutá chyba v Melagenai
Obr. 10 Umístění fotoaparátu a odhadnutá chyba ve Vilniusu (Totoriu 40)
Obr. 11 Ortofoto objektu ve Vilniusu (Totoriu 40): a – z bezpilotního letadla, b – pořízené v roce 1995
Obr. 12 Příklad: a – ortofoto; b – ortografická mapa

ACKNOWLEDGMENTS

This work is funded by the Lithuanian Science Council under the project No. MIP-089/2012.